

$[\text{Ph}_2\text{SnCl}_2\text{F}]^-$ and $[\text{Ph}_2\text{SnClF}_2]^-$ have a lower apicophilicity than the chloride.

Addition of fluoride to Ph_2SnCl_2 or PhSnCl_2 causes phenyl group migration. The degree of phenyl group migration is larger for the monoorganotin(IV) precursors. Interestingly, addition of other Lewis bases such as chloride on bromide ion or triorganylphosphine oxide does not

promote such migration.

Acknowledgment. Financial assistance from the Australian Research Council (ARC) is gratefully acknowledged.

OM920403A

Nature of the Stabilization of a Carbenium Ion Adjacent to Two Organometallic Groups.

$[\text{Mo}_2\text{Cp}_2(\text{CO})_4(\mu\text{-FcCHC}\equiv\text{C}(\text{CH}_2)_2\text{CH}_3)]^+\text{BF}_4^-$: X-ray Structure and NMR Dynamic Investigation

C. Cordier,[†] M. Gruselle,[†] J. Vaissermann,[‡] L. L. Troitskaya,[§] V. I. Bakhmutov,[⊥] V. I. Sokolov,[§] and G. Jaouen^{*†}

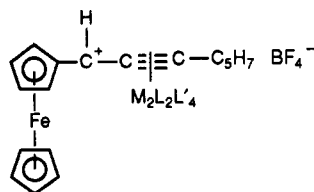
URA 403 CNRS, ENSCP, 11 rue P. et M. Curie, 75231 Paris cédex 05, France, Laboratoire de Chimie des Métaux de Transition, URA 419 CNRS, Université P. et M. Curie, 4 place Jussieu, 75252 Paris cédex 05, France, Laboratory for Organometallic Stereochemistry, INEOS, 28 Vavilov Street, 117813 Moscow, Russian Federation, and NMR Laboratory, INEOS, 28 Vavilov Street, 117813 Moscow, Russian Federation

Received April 13, 1992

A variable-temperature ^{13}C NMR investigation in solution, complemented with a CPMAS experiment in the solid state, was performed on $[\text{Mo}_2\text{Cp}_2(\text{CO})_4(\mu\text{-FcCHC}\equiv\text{C}(\text{CH}_2)_2\text{CH}_3)]^+\text{BF}_4^-$ (1c). In solution, the NMR spectra are highly temperature dependent. We describe fluxional behavior of this carbenium ion simultaneously adjacent to two organometallic groups; ferrocenyl and acetylenic dimolybdenum cluster. In addition, the X-ray structure of the complex 1c was determined. This compound crystallizes in the monoclinic space group $P2_1/n$ with $Z = 4$ and cell dimensions $a = 7.972(2) \text{ \AA}$, $b = 27.221(4) \text{ \AA}$, and $c = 15.285(3) \text{ \AA}$; the structure was refined to R and R_w values of 4.1 and 4.5, respectively, with the use of 2711 reflections. We demonstrate that the dimolybdenum cluster is mainly involved in the stabilization of the positive charge. The fluxional behavior together with molecular structure data shows an uncommon role of the ferrocenyl group in its interaction with the carbenium ion.

Introduction

We have previously described¹ the synthesis of carbenium ions 1a and 1b where the carbon atom bearing the positive charge is simultaneously adjacent to a ferrocenyl group and an acetylenic C_2M_2 cluster. Primary NMR

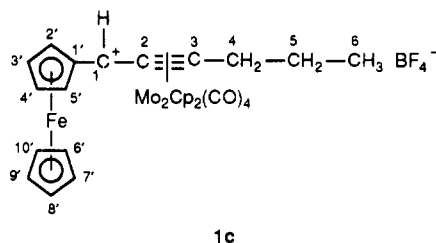


1a: $M = \text{Co}$, $L = L' = \text{CO}$

1b: $M = \text{Mo}$, $L = \text{Cp}$, $L' = \text{CO}$

studies have provided some evidence about the nonfluxionality of the cobalt species 1a and on the contrary the fluxionality of the cation 1b at room temperature, in solution. We had interpreted the behavior of 1b as a competition between the two organometallic groups FeCp_2 and $\text{C}_2\text{M}_2\text{L}_6$ in stabilizing the C^+ . In such a case, the stabilization mode of C^+ is not so easy to display. On the basis of our knowledge about structural properties and flux-

ionality for carbenium ions adjacent to the one organometallic group $\text{C}_2\text{Mo}_2\text{Cp}_2(\text{CO})_4$, we will discuss the stabilization mode for 1c. A variable-temperature NMR



1c

investigation, in solution, completed with a CPMAS and the molecular structure, in the solid state, has been performed on 1c to explain the stabilization and dynamical behavior of this intricate carbenium ion.

Results

Description of the Structure. The X-ray crystal structure of $[\text{Mo}_2\text{Cp}_2(\text{CO})_4(\mu\text{-FcCHC}\equiv\text{C}(\text{CH}_2)_2\text{CH}_3)]^+\text{BF}_4^-$ has been determined. The asymmetric unit consists of four discrete cations $[\text{Mo}_2\text{Cp}_2(\text{CO})_4(\mu\text{-FcCHC}\equiv\text{C}(\text{CH}_2)_2\text{CH}_3)]^+$ and four BF_4^- anions. A solvent molecule, CH_2Cl_2 , is enclosed in the unit cell, but has no direct interaction with

[†] ENSCP.

[‡] Université P. et M. Curie.

[§] Laboratory for Organometallic Stereochemistry, INEOS.

[⊥] NMR Laboratory, INEOS.

(1) Troitskaya, L. L.; Sokolov, V. I.; Bakhmutov, V. I.; Reutov, O. A.; Gruselle, M.; Cordier, C.; Jaouen, G. *J. Organomet. Chem.* 1989, 364, 195.

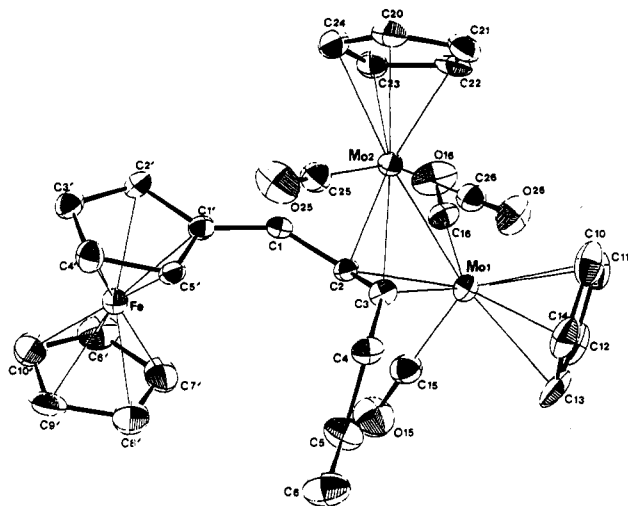


Figure 1. X-ray molecular structure of $[\text{Mo}_2\text{Cp}_2(\text{CO})_4(\mu\text{-FcCHC}\equiv\text{C}(\text{CH}_2)_2\text{CH}_3)]^+$ (1c).

Table I. Crystal Data Collection and Refinement Parameters

chem formula	$\text{C}_{30}\text{H}_{27}\text{O}_4\text{FeMo}_2\text{BF}_4\cdot\text{CH}_2\text{Cl}_2$
fw	800.1
cryst syst	monoclinic
space group	$P2_1/n$
Z	4
a, Å	7.972 (2)
b, Å	27.221 (4)
c, Å	15.285 (3)
β , deg	97.56 (2)
V, Å ³	3288 (8)
F(000)	1728
ρ (calcd), g·cm ⁻³	1.62
μ (Mo K α) cm ⁻¹	12.2
cryst size, mm	0.06 × 0.20 × 0.30
diffractometer	CAD4
monochromator	graphite
radiation	Mo K α (0.71070)
temp, °C	20
scan type	$\omega/2\theta$
scan range θ , deg	$0.8 + 0.34 \tan \theta$
2θ range, deg	3–50
rlfncs collected	5785
reflncs used (criteria)	2711 ($I > 3\sigma(I)$)
R	0.041
R_w^a	0.045
absorption correction ^b	min, 0.90; max, 1.08
secondary ext	no
weighting scheme	unit weights
rms (shift/esd) (last ref)	0.24
ls parameters	495

^a $R_w = [\sum_i W_i(F_o - F_c)^2 / \sum_i W_i F_o^2]^{1/2}$. ^b Difabs: Walker, N.; Stuart, D. *Acta Crystallogr. A* 1983, 39, 159.

the cationic part. The ORTEP plot of one of the crystallographically independent cations present in the unit is shown in Figure 1. Crystal data collection and refinement parameters are collected in Table I. The fractional atomic parameters for each non-hydrogen atom are listed in Table II. Selected bond lengths and angles are presented in Table III (the full data, e.g., interatomic distances, bond angles, and thermal parameters, are available as supplementary material).

The central Mo_2C_2 moiety is quasi tetrahedral and is typical of that found in other acetylene-bridged compounds $[\text{Mo}_2\text{Cp}_2(\text{CO})_4(\mu\text{-RC}\equiv\text{CR})]_2$.² The Mo–Mo bond length (2.963 Å), consistent with a single bond, is slightly shorter

Table II. Fractional Atomic Parameters and Equivalent Isotropic Thermal Parameters (Å²) for 1c

atom	x/a	y/b	z/c	U(eq)
Mo(1)	0.9553 (1)	0.10240 (3)	0.81676 (6)	0.0335
Mo(2)	0.6934 (1)	0.17540 (3)	0.75065 (6)	0.0305
Fe	0.8651 (2)	0.13262 (5)	0.42851 (9)	0.0379
C(1)	0.875 (1)	0.1596 (4)	0.6217 (6)	0.0321
C(2)	0.855 (1)	0.1232 (3)	0.6864 (6)	0.0306
C(3)	0.733 (1)	0.0965 (4)	0.7193 (6)	0.0315
C(4)	0.615 (1)	0.0553 (4)	0.6887 (8)	0.0395
C(5)	0.700 (2)	0.0125 (5)	0.650 (1)	0.0547
C(6)	0.574 (2)	-0.0278 (6)	0.619 (1)	0.0695
C(1')	0.781 (1)	0.1635 (3)	0.5344 (6)	0.0312
C(2')	0.814 (1)	0.2008 (4)	0.4740 (7)	0.0401
C(3')	0.710 (1)	0.1905 (4)	0.3933 (7)	0.0442
C(4')	0.614 (2)	0.1493 (5)	0.4034 (7)	0.0480
C(5')	0.654 (1)	0.1312 (4)	0.4909 (6)	0.0321
C(6')	1.115 (2)	0.1299 (5)	0.4115 (9)	0.0590
C(7')	1.079 (2)	0.0937 (5)	0.4703 (8)	0.0560
C(8')	0.955 (2)	0.0638 (5)	0.4269 (8)	0.0584
C(9')	0.914 (2)	0.0801 (5)	0.3381 (9)	0.0539
C(10')	1.017 (2)	0.1224 (5)	0.3329 (9)	0.0633
C(10)	0.863 (2)	0.0971 (6)	0.9563 (9)	0.0612
C(11)	1.039 (2)	0.1034 (6)	0.9677 (8)	0.0612
C(12)	1.114 (2)	0.0634 (5)	0.9311 (8)	0.0556
C(13)	0.982 (2)	0.0302 (5)	0.8984 (9)	0.0518
C(14)	0.830 (2)	0.0515 (5)	0.9150 (9)	0.0567
C(20)	0.568 (2)	0.2495 (4)	0.7700 (9)	0.0500
C(21)	0.659 (2)	0.2370 (4)	0.8516 (8)	0.0493
C(22)	0.836 (1)	0.2379 (4)	0.8410 (8)	0.0415
C(23)	0.845 (1)	0.2492 (4)	0.7519 (7)	0.0426
C(24)	0.682 (2)	0.2571 (4)	0.7100 (8)	0.0484
C(15)	1.097 (1)	0.0680 (4)	0.7401 (7)	0.0467
O(15)	1.182 (1)	0.0477 (4)	0.6976 (6)	0.0731
C(16)	1.106 (1)	0.1605 (4)	0.8100 (7)	0.0393
O(16)	1.199 (1)	0.1910 (3)	0.8096 (6)	0.0627
C(25)	0.493 (1)	0.1646 (4)	0.6614 (7)	0.0483
O(25)	0.368 (1)	0.1585 (4)	0.6153 (6)	0.0685
C(26)	0.560 (1)	0.1360 (4)	0.8299 (7)	0.0444
O(26)	0.481 (1)	0.1147 (3)	0.8707 (5)	0.0552

Table III. Selected Bond Lengths (Å) and Angles (deg) for 1c

Mo(1)–Mo(2)	2.963 (1)	Mo(2)–C(1)	2.63 (1)
Mo(1)–C(2)	2.122 (9)	Mo(1)–C(3)	2.165 (9)
Mo(2)–C(2)	2.233 (9)	C(1)–C(1')	1.45 (1)
Mo(2)–C(3)	2.23 (1)	C(2)–C(3)	1.36 (1)
C(1)–C(2)	1.42 (1)	C(16)–O(16)	1.11 (1)
C(15)–O(15)	1.14 (1)	C(26)–O(26)	1.11 (1)
C(25)–O(25)	1.15 (1)	Fe–C(2')	2.04 (1)
Fe–C(1')	2.015 (9)	Fe–C(4')	2.04 (1)
Fe–C(3')	2.03 (1)	Fe–C(6')	2.05 (1)
Fe–C(5')	2.04 (1)	Fe–C(8')	2.01 (1)
Fe–C(7')	2.04 (1)	Fe–C(10')	2.04 (1)
Fe–C(9')	2.06 (1)		
C(1')–C(1)–C(2)	126.7 (9)	C(2)–Mo(1)–Mo(2)	48.7 (2)
Mo(2)–C(25)–O(25)	174.2 (10)	C(3)–Mo(1)–C(2)	37.1 (3)
Mo(2)–C(26)–O(26)	177.0 (10)	C(3)–Mo(1)–Mo(2)	48.6 (3)
Mo(1)–C(15)–O(15)	178.2 (10)	C(3)–Mo(2)–Mo(1)	46.7 (2)
Mo(1)–C(16)–O(16)	175.0 (9)	C(2)–Mo(2)–Mo(1)	45.6 (2)
C(1)–C(2)–Mo(2)	89.2 (6)	C(3)–Mo(2)–C(2)	35.5 (3)
C(25)–Mo(2)–C(26)	83.9	C(15)–Mo(1)–C(16)	87.2

than that observed in the primary cation 2a isolated by Curtis.³ The interatomic distance Mo–C⁺ (Mo(2)–C(1)) is short enough (2.63 Å) to involve an electronic interaction between the d-orbital system of the metallic atom Mo and the p-orbital of the positively charged carbon. The C(2)–C(3) distance (1.36 Å) is in agreement with those characterized for cations adjacent to the unit $\text{C}_2\text{Mo}_2\text{Cp}_2(\text{CO})_4$.^{3,4} Three CO ligands are terminal, while one is semibridged to the molybdenum atom to which it is not

(2) Bailey, W. I.; Chisholm, M. H.; Cotton, F. A.; Rankel, L. A. *J. Am. Chem. Soc.* 1978, 100, 5764.

(3) Meyer, A.; McCabe, D. J.; Curtis, D. *Organometallics* 1987, 6, 1491.

(4) Gruselle, M.; Cordier, C.; Salmain, M.; El Amouri, H.; Guérin, C.; Vaissermann, J.; Jaouen, G. *Organometallics* 1990, 9, 2993.

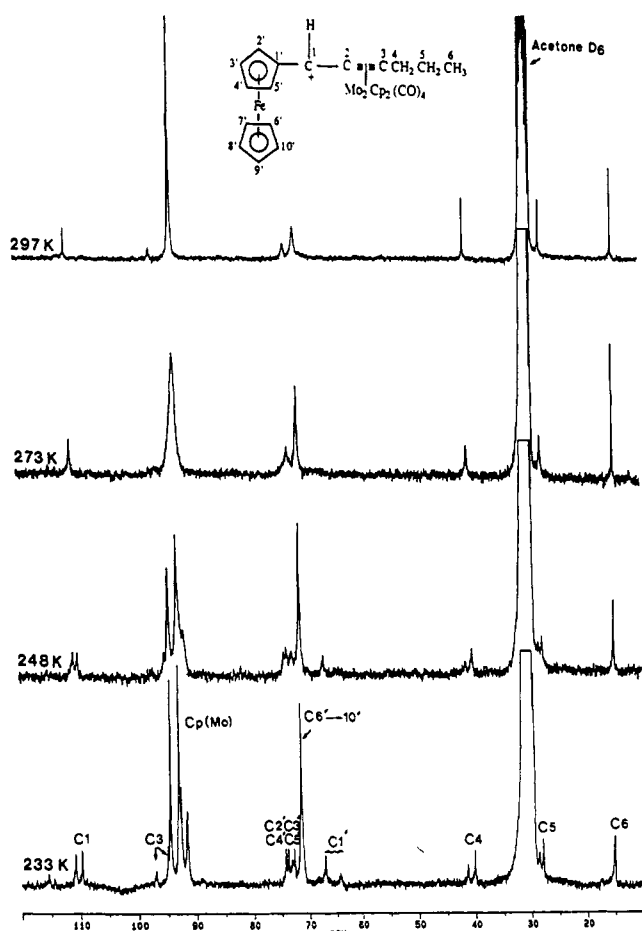


Figure 2. Variable-temperature ^{13}C NMR spectra of **1c** in acetone- d_6 .

directly coordinated. The lack of a $\nu(\text{CO})$ band below 1900 cm^{-1} , typical of semibridging carbonyls, suggests that the semibridging posture is very weak in **1c**. Lack of any local symmetry in the arrangement of the ligands around the C_3Mo_2 core is noticed. The symmetry of the ferrocenyl group is extremely close to D_{5h} symmetry. The two cyclopentadienyl rings of this moiety are eclipsed and parallel. The substituted ring has no distortion. A very weak bending of $\text{C}(1)^+$ down toward the Fe atom is observed. However, this bending is too small to have a structural significance. The distance between these two atoms does not allow a direct interaction. The $\text{C}(1)\text{---}\text{C}(1')$ interatomic distance (1.45 \AA) is consistent with some double bond $\text{C}=\text{C}$ feature.

NMR Spectra. In solution, assignment of the proton signals with CD_3COCD_3 as solvent is mentioned in a previous paper.¹ The $^{13}\text{C}\{^1\text{H}\}$ chemical shifts have been assigned by analogy to the previous work and are listed in Table IV. As shown in Figure 2, the ^{13}C NMR spectrum in CD_3COCD_3 is highly temperature dependent in the temperature range 213–297 K.

At room temperature, the ^{13}C NMR spectrum morphology is consistent with a molecule without a chiral center in its structure, on the time scale of the NMR measurements. In the region of the Cp(Mo) resonances, one signal in the ^{13}C NMR spectrum is observed for the cyclopentadienyl groups coordinated to Mo atoms at 297 K. As the temperature is lowered, two signals appear with different intensity, and then, on further lowering of temperature, four signals are displayed with different intensities at 233 K (Figure 3a). These two pairs of signals indicate the existence of two diastereoisomers, the ratio of population being about 2:1. We note that every carbon

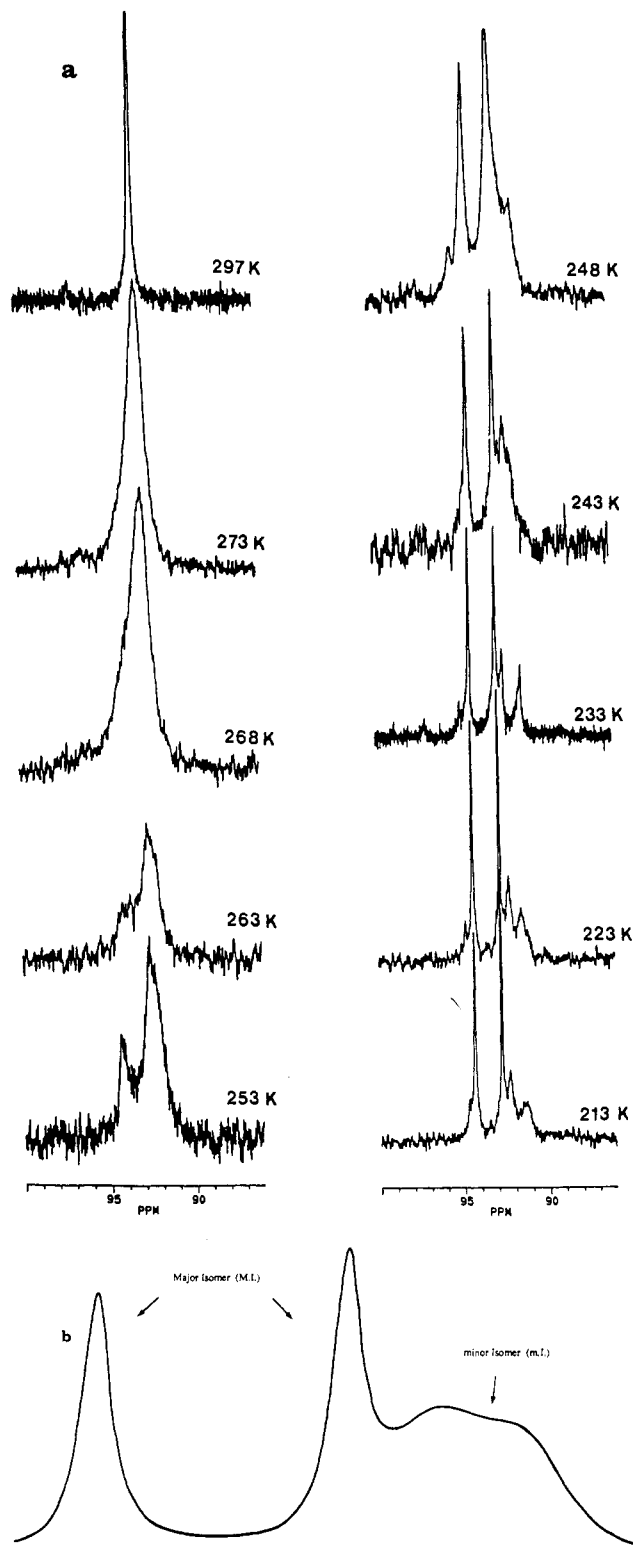


Figure 3. (a) Variable-temperature ^{13}C NMR spectra of **1c** in acetone- d_6 in the region of the Cp(Mo) resonances. (b) ^{13}C NMR spectrum simulation of the Cp(Mo) resonance for **1c** at 243 K.

appears as two signals at 233 K (Figure 2) except those of unsubstituted Cp coordinated to Fe ($\text{C}(6') \rightarrow \text{C}(10')$). It means that lowering the temperature stops two different dynamic processes.

The situation is the same in the ^1H NMR spectrum in the region of the Cp(Mo) resonances as shown in Figure 4. But it is clear that a solvent effect acts on the energy barrier of the processes and especially on the lowest energy fluxional process. For instance, in CD_3COCD_3 , four

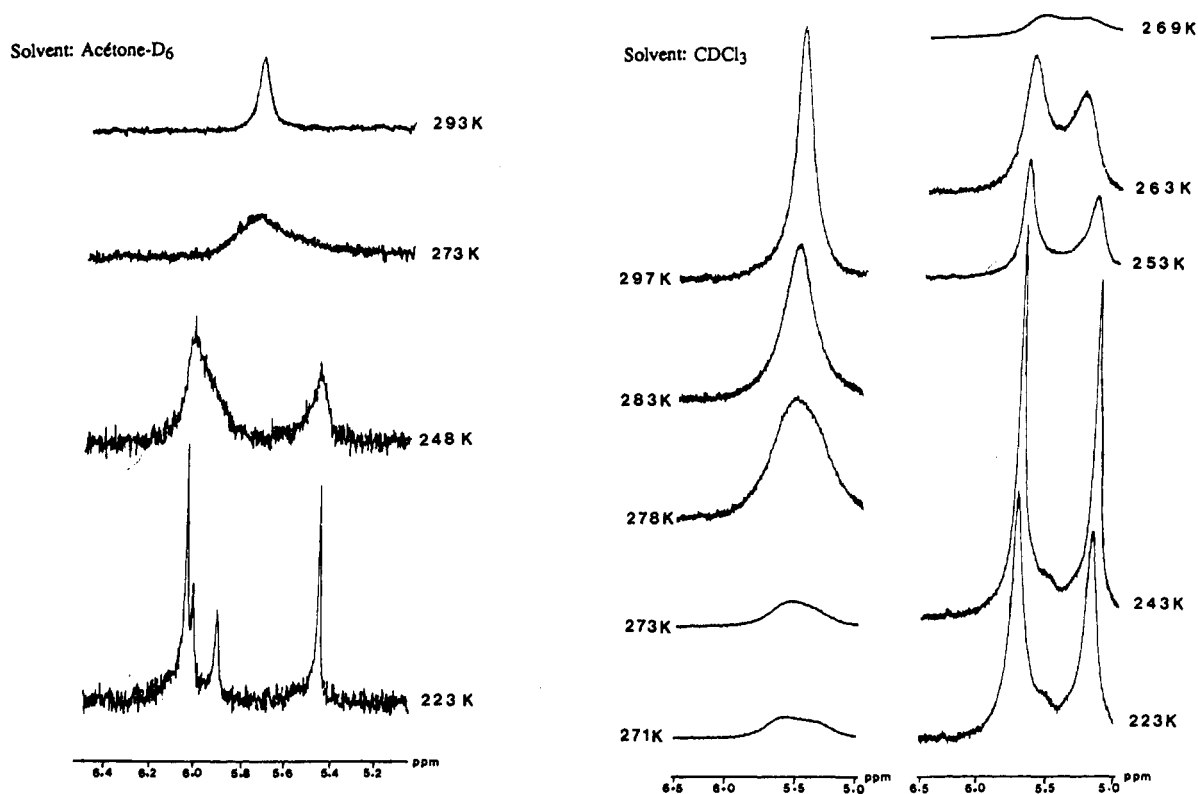


Figure 4. Variable-temperature ^1H NMR spectra of **1c** in acetone- d_6 and CDCl_3 in the region of the Cp(Mo) resonances.

Table IV. Carbon NMR Chemical Shifts for **1c** (ppm)

atoms	$^{13}\text{C}\{^1\text{H}\}$ in CD_3COCD_3		^{13}C CPMAS
	297 K	223 K	
1	111.37	109.68 110.79	111.56
2	<i>a</i>	<i>a</i>	86.93
3	96.60	94.92 97.42	93.6
4	40.99	40.04 41.35	<i>a</i>
5	27.57	27.81 28.52	<i>a</i>
6	14.72	14.90 14.92	16.42
1'	<i>a</i>	67.03 64.04	67.00
2', 3', 4', 5'	73.36	74.19 73.74 72.67 73.10	73.30 ^b
6', 7', 8', 9', 10'	71.60	71.31	70.84
Cp(Mo)	93.10	94.34 92.80 92.44 91.40	91.82
CO(Mo)	<i>a</i>	<i>a</i>	222.72 ^b 212.50 ^b

^aSignal not observed. ^bBroad signal.

well-resolved signals are observed at 223 K whereas only two resolved signals appear in CDCl_3 at the same temperature.

The ^{13}C NMR spectra for **1c** in both solution and the solid state are almost identical, the difference in chemical shift values being less than 2 ppm. Consequently, we postulate that one of the two diastereomers has the same structure as the one depicted in the ORTEP view.

Discussion

Literature precedents report many examples of a carbenium ion adjacent to only one ferrocenyl group⁵

or to only one acetylenic dimolybdenum cluster.^{3,4} Researchers have noticed the remarkable stabilization of such carbenium ions. They conclude that the stabilization is the result of an interaction between the p-orbital of the positively charged carbon and the d-orbital system of the molybdenum or iron metallic atom.

Let us examine for each of these two cases, the stabilization of the carbenium ion (1) adjacent to a dimolybdenum cluster and (2) adjacent to a ferrocenyl group and the influence of the stabilization on the dynamic behavior of the cation in solution.

Carbenium Ion Adjacent to Only One Dimolybdenum Cluster. In a previous work,³ Curtis discussed the stabilization and the dynamic processes of the primary cation **2a**. In this compound a strong Mo-C⁺ interaction exists (interatomic distance in the solid state 2.45 Å). EHT calculations⁶ on the derivative cation **2b** promote the evidence of an electronic interaction between Mo and C⁺. This electronic interaction produces chirality in the cluster itself, and leads H(a) and H(b) to be magnetically inequivalent. At room temperature, Curtis mentioned the nonfluxionality of **2a** in solution. At 348 K, a dynamical process interconverts the Cp groups but not H(a) and H(b). Barinov and al.⁷ have studied cations of the C_2Mo_2 series and have observed a second process

(5) a) Nicholas, K. M.; Nestlé, M. O.; Seyferth, D. In *Transition Metal Organometallics in Organic Synthesis*; Alper, H., Ed.; Academic: New York, 1978; Vol. 2 p 1. b) Watts, W. E. *Journal of Organometallic Chemistry Library*; Elsevier: Amsterdam, 1979; Vol. 7, p 399. c) Cais, M. *Organomet. Chem. Rev.* 1966, 1, 435. d) Richards, J. H.; Hill, E. A. *J. Am. Chem. Soc.* 1959, 81, 3484. e) Pettit, R.; Maynes, W. L. In *Carbonyl Ions*; Olah, G. A., Schleyer, P. von R., Eds.; Wiley: New York, 1976; Vol. 5, p 2263. f) Koridze, A. A. *Usp. Khim.* 1986, 2, 277. g) Jaouen, G. *Pure Appl. Chem.* 1986, 58, 597.

(6) Cordier, Ch. Ph.D. Thesis, - P. and M. Curie University, Paris, 1991.

(7) a) Barinov, I. V.; Reutov, O. A.; Polyakov, A. V.; Yanovsky, A. I.; Struchkov, Yu T.; Sokolov, V. I. *J. Organomet. Chem.* 1991, C24, 418. b) Galakhov, M. V.; Bakhmutov, V. I.; Barinov, I. V. *Magn. Res. Chem.*, submitted for publication.

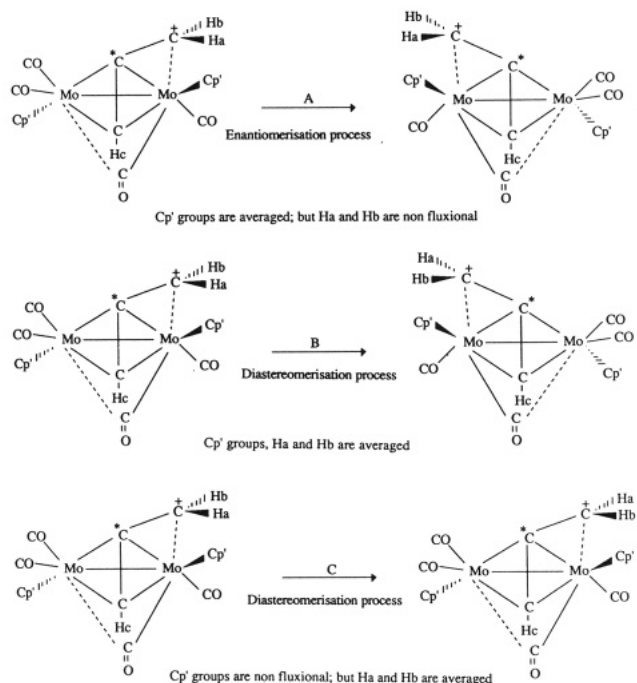
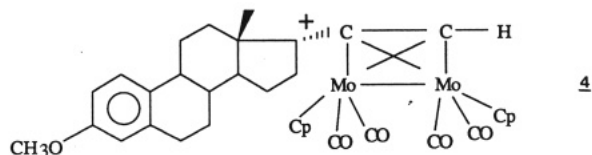
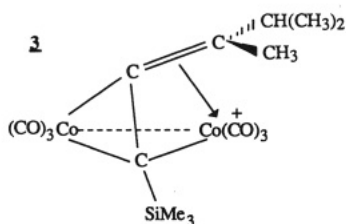
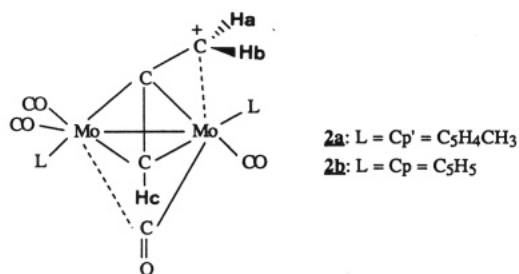


Figure 5. Proposed isomers resulting from the dynamical processes A, B, or C applied to the Curtius cation **2a**.

Chart I



at higher temperature (368 K). They have noticed H(a) and H(b) being fluxional.

Three mechanisms to explain the dynamical solution behavior of these ions have been proposed previously.⁸ They are (A) simultaneous rotation/antarafacial migration, (B) simultaneous rotation/suprafacial migration, and (C)

(8) Cordier, C.; Gruselle, M.; Jaouen, G.; Bakmutov, V. I.; Galakhov, M. V.; Troitskaya, L. L.; Sokolov, V. I. *Organometallics* 1991, 10, 2303.

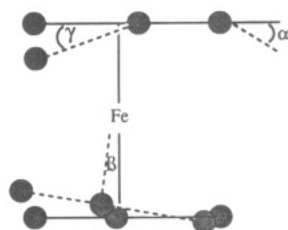


Figure 6. Distortions from the D_{5h} symmetry of an ideal ferrocene (perpendicular view to the C_5 axis of the ferrocene unit).

Table V. Parameters of Distortions from the Ideal Ferrocene for α -Ferrocenyl Cations

carbenium ion	α , deg	β , deg	γ , deg	Fe-C ⁺ distance, Å	ref
C ₂₅ H ₁₉ Fe (5)	14.6	2.7	<i>a</i>	2.957	14
C ₂₃ H ₁₉ Fe (6)	20.7	9.3	9	2.715	13
1c	4	0	0	3.030	this work

^a Unknown value.

simple C-C bond rotation about C⁺-cluster bond. The three associated transition states have been depicted. The effect of each of these mechanisms applied to **2a** is shown in Figure 5.

Consequently, the lowest energy process observed by Curtis on **2a** is the enantiomerization process A. The second mechanism is a diastereomerization which acts on **2b** at 368 K. Cation **3**, studied by Schreiber,⁹ presents the same dynamical behavior, the two processes (enantiomerization and diastereomerization) occurring with the same order (Chart I). We have demonstrated⁸ a different situation for **4**. Diastereomerization process C or B is energetically lower than the enantiomerization A. For this cation, the C⁺-Mo interaction is weakened because of the presence of a bulky steroidal substituent. In fact, the strength of the Mo-C⁺ interaction is directly correlated to the interatomic distance $d(\text{Mo}-\text{C}^+)$ determined by X-ray analysis. For instance, in **2b** $d(\text{Mo}-\text{C}^+) = 2.44$ Å compared to that found for **4** ($d(\text{Mo}-\text{C}^+) = 2.76$ Å). The fluxionality of these species is dependent on the strength of the metal-C⁺ interaction.

Carbenium Ion Adjacent to Only One Ferrocenyl Group. Stabilization of the carbenium ion center in α -metallocenyl cations has been a well-established fact for decades.¹⁰ Attention has been largely concentrated on α -ferrocenyl systems with a lot of experimental facts taken from synthetic, stereochemical, NMR spectroscopic, and structural studies.¹¹ The main topic discussed was the direct participation of the metal orbitals with an empty p-orbital of α -C⁺. The current view is that the extent of direct participation of the metal depends strongly of the molecular structure. Gleiter and Seeger¹² have demonstrated by calculations on the ferrocenylmethyl cation that the metal orbital participation in the bonding and stabilization of C⁺ is accompanied by various distortions of the ferrocenyl moiety. In particular, three distortions from D_{5h} symmetry have been predicted by Gleiter and Seeger

(9) Schreiber, S. L.; Klimas, M. T.; Sammakia, T. *J. Am. Chem. Soc.* 1987, 109, 5749.

(10) a) Richards, J. H.; Hill, E. A. *J. Am. Chem. Soc.* 1959, 81, 3484. b) Hill, E. A.; Richards, J. H. *J. Am. Chem. Soc.* 1961, 83, 3840. c) Hill, E. A.; Richards, J. H. *J. Am. Chem. Soc.* 1961, 83, 4216. d) Trifan, D. S.; Backsai, R. *Tetrahedron Lett.* 1960, 13, 1.

(11) a) Traylor, T. G.; Ware, J. C. *J. Am. Chem. Soc.* 1967, 89, 2304. b) Watts, W. E. *J. Organomet. Chem. Libr.* 1979, 7, 399. c) Sokolov, V. I. *Chirality and Optical Activity in Organometallic Compounds*; Gordon & Breach: London, 1992.

(12) Gleiter, R.; Seeger, R. *Helv. Chim. Acta* 1971, 54, 1217.

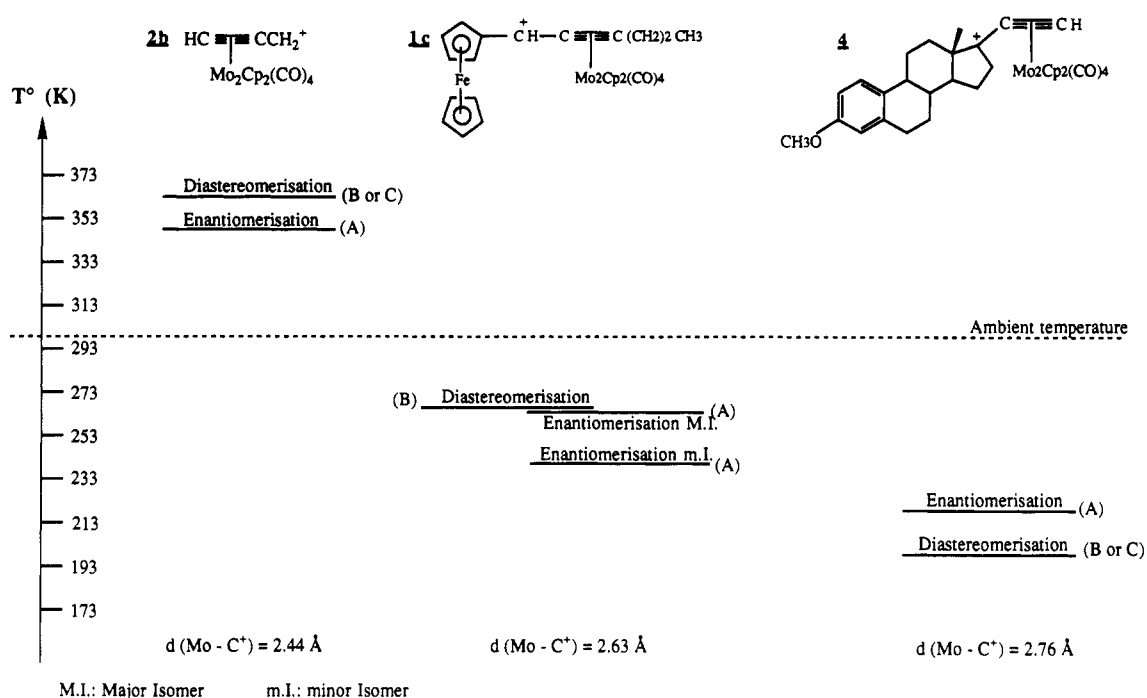


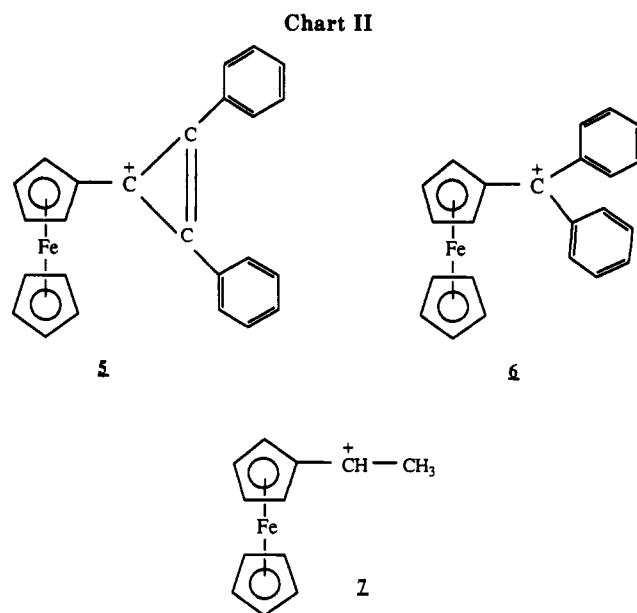
Figure 7. Activation barrier energy of the dynamical processes A, B, or C as a function of the strength of the Mo-C⁺ interaction in 2b, 1c, and 4.

(Figure 6). The calculated angles found by these researchers are $\alpha = 40^\circ$ (Gleiter and Seeger admitted that this value could be too large), $\beta = 10^\circ$, and $\gamma = 0^\circ$.

In the literature, two structures of α -ferrocenyl cations have been published.^{13,14} They are in agreement with some participation of the iron in stabilization of the carbenium center. A few essential parameters are summarized in Table V. The ferrocenyldiphenylcarbenium ion 6 (Chart II) can be regarded as an archetype of ion stabilized by Fe.¹³ Indeed, in this structure, aromatic rings are not conjugated to each other. Consequently, the π -electron system of these rings does not stabilize the carbenium ion center. In such an example, the Fe-C⁺ interaction is important.

It is well known that optical activity is preserved when enantiomeric CpMCpCH*(OH)R will give rise to carbenium ion and then restore the initial carbinol, the stereochemical stability being higher for Ru than Fe.¹⁵ The immediate reason is the high barrier for rotation around the MCP-C⁺ whichever the underlying base would be. In agreement, we have demonstrated previously¹ that a chiral center persists at room temperature in the case of the carbenium ion adjacent to both the ferrocenyl group and a propargylic dicobalt cluster.

Nature of Stabilization of C⁺ for 1c. The set of spectroscopic and structural results obtained for 1c compared to those discussed previously for a carbenium ion center adjacent to only one organometallic moiety is in agreement with a strong participation of the molybdenum cluster. In solution, the ¹³C NMR spectrum is highly temperature dependent (Figures 2 and 3a). At room temperature, 1c is fluxional. Lowering the temperature from 297 to 233 K stops dynamic processes as shown Figure 3a. According to spectral simulation by the DNMR5 program, the highest energy process is the diastereomerization



process B (Figure 3b). The diastereomerization process stop leads to two isomers in solution with different population. Almost at the same temperature, the enantiomerization process A stops for the major isomer. But this process occurs at lower temperature for the minor isomer (243 K).

The enantiomerization process stop could be the result of a Fe-C⁺ interaction. But in the solid state, the distance $d(\text{Fe}-\text{C}^+)$ (3.03 Å) is too long to explain such a stabilization mode of C⁺, as seen in Table II. In solution, the molecular structure of 1c is very similar to that in the solid state (ORTEP view) as predicted by NMR data (¹³C NMR and CPMAS). Consequently, we postulate that the stabilization mode for 1c is essentially due to Mo cluster participation. The interatomic distance $d(\text{Mo}-\text{C}^+)$ in 1c is intermediate between those observed for 2b and 4. In Figure 7, we have illustrated the effect of the strength of the Mo-C⁺ interaction on the activation barrier energy of the

(13) Behrens, U. *J. Organomet. Chem.* 1979, 182, 89.

(14) Sime, R. L.; Sime, R. J. *J. Am. Chem. Soc.* 1974, 96, 892.

(15) a) Turbitt, T. D.; Watts, W. E. *J. Chem. Soc., Perkin Trans. 2* 1974, 177. b) Nefedova, M. N.; Mamedyavova, I. H.; Petrovski, P. V.; Sokolov, V. I. *J. Organomet. Chem.*, in press.

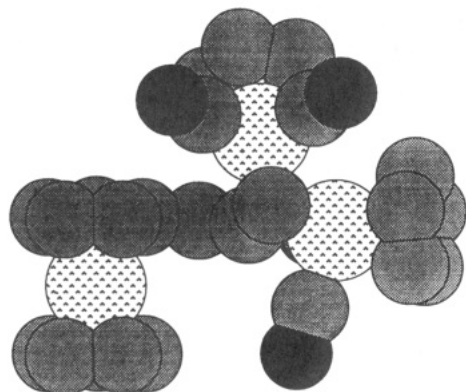


Figure 8. View of the X-ray crystal structure of **1c** without the alkyl chain (e.g., C(4), C(5), C(6), and hydrogen atoms are not plotted). It shows the planar geometry of the ferrocenyl moiety and the possibility of conjugation between the substituted Cp(Fe) ring and the C⁺.

different processes. It is clear that the fluxionality of these cations is directly correlated to the interatomic distance $d(\text{Mo}-\text{C}^+)$.

This interpretation leaves a question unresolved: what role does the ferrocenyl group play? The comparison with the structures of **5** and **6** is very interesting (see Table V). Indeed, on the basis of the X-ray parameters, it seems that the iron atom does not participate directly in the stabilization of C⁺ for **1c** in opposition to the two other structures published. Nevertheless, the Mo-C⁺ interaction is weaker than that of **2b**. This situation can be interpreted in two ways: in terms of steric hindrance as observed for **4** and in terms of electronic factors, e.g., conjugation between the π -electron system of the substituted ferrocenyl Cp and the p-orbital on C⁺.

The first possibility is not very convincing for many reasons. First, the coalescence of ¹³C signals for the substituted Cp(Fe) and for the Cp(Mo) occurs at the same temperature. This indicates the unity of the process. Second, the semibridging CO ligand in **1c** is similar to that of the primary cation **2b** which has no special steric hindrance. In the bulky cation **4**, because of the crowding, one CO group is forced into the region close to the Mo-Mo bond and the semibridging posture is more significant. This particularity has been described by Cotton et al.² for the molecules Mo₂Cp₂(CO)₄(μ -RC≡CR') and is the evidence of an internal crowding in the molecules.

The second explanation is based on the possibility of conjugation between the HOMO π -orbital located on the substituted Cp(Fe) ring and the LUMO p-orbital on C⁺. In the literature,^{13,14} the researchers exclude this possibility on the basis of direct interaction between the d_{z²}-orbital of Fe and the LUMO p-orbital on C⁺. But for **1c**, the planar geometry of the ferrocenyl moiety allows a direct overlap of the two systems of orbitals: the HOMO π -orbital on the Cp(Fe) ring and the LUMO p-orbital on C⁺ (as shown in Figure 8). Consequently, the delocalization of the positive charge on the Cp(Fe) ring decreases the residual charge on the carbon C(1) and is in agreement with the weakness of the Mo-C⁺ interaction. The ¹³C NMR chemical shifts published previously¹ show a remarkable upfield shift of C(1') in **1c** compared either to the derivative alcohol or to the α -ferrocenyl cation **7** which constitutes a good model for a Fe-C⁺ direct interaction. It involves a strong electronic density around the bond C(1')-C(1) which is consistent with the interatomic distance observed in the solid state. This set of observations (e.g., NMR data, fluxionality, and structural properties)

leads us to conclude that **1c** is an unusual case where the ferrocenyl group participates in the stabilization of the C⁺ center by its substituted ring π -system.

Conclusion

Our NMR results together with molecular structure data have shown the competition between the ferrocenyl group and the dimolybdenum acetylenic cluster to stabilize the adjacent cation center. While the dimetallic cluster is the main contributor to the stabilization and involves the fluxional behavior of the molecule, the ferrocenyl group seems also to participate with its π -electronic system located on the substituted ring. Fluxional processes of the carbenium ions adjacent to dimolybdenum acetylenic clusters are correlated with the strength of the Mo-C⁺ interaction which is the result of an electronic interaction between an occupied d-orbital of Mo and the vacant p-orbital on C⁺.

Experimental Section

The synthesis of the carbenium ion **1c** and its precursor alcohol is similar to the synthesis of **1b** fully described in a previous work.¹ The cation was obtained as a dark violet powder. Single violet crystals were grown from a mixture of CH₂Cl₂/ether by slow evaporation at room temperature. Solvents were purified and dried prior to use by conventional distillation techniques under argon. A suitable crystal was selected for X-ray diffraction.

Crystal Data for C₃₀H₂₇O₄FeMo₂BF₄·CH₂Cl₂. Intensity data were collected at room temperature on a Nonius CAD4 diffractometer using Mo K α radiation. The accurate cell dimensions and orientation matrix were obtained from least-squares refinements of the setting angles of 25 well-defined reflections. No decay in the intensities of two standard reflections was observed during the course of data collection. Complete crystal data and crystal data parameters are listed in the supplementary material. The usual corrections for Lorentz and polarization effects were applied. An empirical absorption correction (DIFABS)¹⁶ was applied (maximum correction 1.08, minimum correction 0.90).

Computations were performed by using CRYSTALS¹⁷ adapted to a Microvax-II computer. Scattering factors and corrections for anomalous dispersions were from ref 18. The structure was resolved by a direct method (SHELXS)¹⁹ and refined by least squares with anisotropic thermal parameters for all non-hydrogen atoms. Hydrogen atoms were located on a difference Fourier map and refined with an overall refinable isotropic thermal parameter.

NMR Experiments. All NMR solution spectra were recorded on a Bruker AM 250 spectrometer. The solvents used were acetone-*d*₆ (¹³C NMR and ¹H NMR) and CDCl₃ (¹H NMR). In Table IV, chemical shifts are reported in parts per million relative to TMS using the residual solvent (CO) at 206 ppm as internal reference. Carbon variable-temperature spectra were acquired at 62.896 MHz using a 10-mm ¹³C probe. Proton spectra were acquired at 250.133 MHz using a 5-mm dual-frequency ¹H/¹³C probe. ¹H NMR spectra recorded in CDCl₃ were obtained in 128 scans in 16K data points over a 2.00-kHz spectral width (4.0-s acquisition time). For the experiments in acetone-*d*₆, the spectral width was increased to 2.50 kHz (3.2-s acquisition time). The ¹³C{¹H} NMR variable-temperature experiments were obtained by using the standard pulse sequence. They result from 1500 scans in 32K data points over a 15.625-kHz spectral width (1.024-s acquisition time). A 2.0-s relaxation delay was used. Temperatures mentioned in Figures 2-4 are known with an accuracy of ± 2 K. Solid-state ¹³C spectra were recorded on a Bruker CXP

(16) Walker, N.; Stuart, D. *Acta Crystallogr.* 1983, A39, 159.

(17) Watkin, D. J.; Carruthers, J. R.; Betteridge, P. W. *CRYSTALS User Guide*; Chemical Crystallography Laboratory, University of Oxford: Oxford, England, 1986.

(18) *International Tables for X-Ray Crystallography*; Kynoch Press: Birmingham, England, 1974; Vol. IV.

(19) Sheldrick, G. M. *SHELXS86, Program for Crystal Structure Solution*; University of Göttingen: Göttingen, 1986.

200 instrument at $T^\circ = 298$ K. The standard PENMR method, including a rotation frequency of the sample of 2500 Hz, was used. The contact time introduced was 5 ms.

Acknowledgment. This work results from a cooperation between CNRS and the Academy of Sciences of the Russian Federation.

Supplementary Material Available: Full tables of data collection parameters, atomic fractional parameters, hydrogen fractional parameters, anisotropic thermal parameters, and bond distances and angles (8 pages). Ordering information is given on any current masthead page.

OM920204R

Synthesis of $\text{Os}_3(\text{CO})_{10}(\text{CNR})(\text{NCMe})$ and Its Reaction with Propynoic Acid

Kuang-Lieh Lu,^{*†} Chi-Jung Su,^{†‡} Yen-Wen Lin,^{†‡} Han-Mou Gau,[‡] and Yuh-Sheng Wen[†]

*Institute of Chemistry, Academia Sinica, Taipei, Taiwan, Republic of China,
and Department of Chemistry, National Chung-Hsing University, Taichung, Taiwan, Republic of China*

Received March 9, 1992

The nitrile derivatives $\text{Os}_3(\text{CO})_{10}(\text{CNR})(\text{NCMe})$ (**2**) have been prepared by the reaction of isocyanide complexes $\text{Os}_3(\text{CO})_{11}(\text{CNR})$ (**1**) with Me_3NO in the presence of CH_3CN . The labile complex **2** on reaction with two-electron donor ligands L (L = CO, PPh_3 , PMePh_2) gives $\text{Os}_3(\text{CO})_{10}(\text{CNR})\text{L}$ (**3**). Treatment of **2** with propynoic acid ($\text{HC}\equiv\text{CCO}_2\text{H}$) in CH_2Cl_2 yields the hydrido complexes $(\mu\text{-H})\text{Os}_3(\text{CO})_{10}(\mu_2\text{-OCOC}\equiv\text{CH})(\text{CNR})$ (**4**); however, complex **2** reacts with propynoic acid in acetonitrile to form complex **4** and the bridging aminocarbyne species $\text{Os}_3(\text{CO})_{10}(\mu_2\text{-OCOC}\equiv\text{CH})(\mu_2\text{-C}\equiv\text{NHR})$ (**5**) containing a unique bridging unidentate $(\mu_2\text{-}\eta^1\text{-oxo})$ carboxylate ligand. Molecular structures of $\text{Os}_3(\text{CO})_{10}(\text{CNPr})(\text{PPh}_3)$ (**3a**) and $\text{Os}_3(\text{CO})_{10}(\mu_2\text{-OCOC}\equiv\text{CH})(\mu_2\text{-C}\equiv\text{NHR})$ (**5a**) have been determined by X-ray diffraction studies. Crystal data are as follows. **3a**: $P\bar{1}$; $a = 11.4611$ (14), $b = 11.6963$ (19), $c = 14.9661$ (22) Å; $\alpha = 93.635$ (12), $\beta = 73.633$ (11), $\gamma = 117.325$ (11)°; $V = 1705.0$ (4) Å³, $Z = 2$; $R = 4.2\%$, $R_w = 5.1\%$. **5a**: $P2_12_12_1$; $a = 9.4241$ (23), $b = 15.414$ (4), $c = 15.972$ (3) Å; $V = 2320.2$ (9) Å³, $Z = 4$; $R = 3.2\%$, $R_w = 3.5\%$.

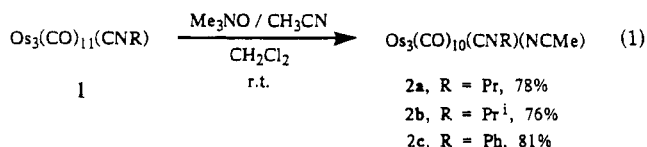
Introduction

Isocyanides are known to be isoelectronic with CO,¹ and it is of interest to learn the effect of replacement of carbonyl ligands with isocyanide on the reactivity of metal carbonyl complexes. Although the coordinated isocyanide has been demonstrated to be capable of reacting with a hydrogen atom to form a bridging formimidoyl or a bridging aminocarbyne ligand in the osmium cluster sphere,² this aspect of chemistry has not been extensively studied probably due to the relatively difficult preparation of the osmium isocyanide cluster. Recently we have reported a high-yield route to the synthesis of the osmium isocyanide clusters $\text{Os}_3(\text{CO})_{11}(\text{CNR})$ by the reaction of $\text{Os}_3(\text{CO})_{12}$ with phosphine imides.³ Considering the importance of oxy ligands of various sorts in the chemical modification of CO in a cluster or on a surface,^{4,5} we therefore started to study the interactions of the osmium isocyanide complexes with Brønsted acids in order to examine the transformation or coordination behavior of the oxy and isocyanide ligands in trinuclear osmium clusters. In this paper, we report the preparation of the labile nitrile complexes $\text{Os}_3(\text{CO})_{10}(\text{CNR})(\text{NCMe})$ and their reactions with propynoic acid. The features of these reactions are the transformation of the isocyanide ligand and the unique bridging unidentate coordination mode $(\mu_2\text{-}\eta^1\text{-O})$ of the carboxylate ligand in the cluster sphere.

Results and Discussion

Preparation of Acetonitrile Complexes $\text{Os}_3(\text{CO})_{10}(\text{CNR})(\text{NCMe})$. Treatment of the osmium isocyanide complexes $\text{Os}_3(\text{CO})_{11}(\text{CNR})$ (**1**) in CH_2Cl_2 with Me_3NO in

the presence of CH_3CN at room temperature yields the acetonitrile complexes $\text{Os}_3(\text{CO})_{10}(\text{CNR})(\text{NCMe})$ (**2a**, R = Pr; **2b**, R = Prⁱ; **2c**, R = Ph) in good yield (eq 1). The



reactions were monitored by IR spectroscopy by following the disappearance of ν_{CO} bands of the starting material, $\text{Os}_3(\text{CO})_{11}(\text{CNR})$. In general, slightly more than a stoichiometric amount of Me_3NO was required. The yellow complexes $\text{Os}_3(\text{CO})_{10}(\text{CNR})(\text{NCMe})$ are "lightly stabilized" in CH_2Cl_2 solution and decompose slowly to light green materials, but they are stable in the presence of acetonitrile and can be recrystallized from a mixture of hexane/ CH_2Cl_2 / CH_3CN . The infrared spectrum of **2c** shows the $\nu_{\text{C}\equiv\text{N}}$ absorption at 2160 cm^{-1} , which is characteristic of terminally coordinated isocyanide ligand.² The FAB mass spectrum of **2c** shows the molecular ion at m/z 997 as well as the subsequent CO-lost fragments. In addition to the appropriate isocyanide ligand ¹H NMR resonance, each derivative displays one intense signal for the methyl group of acetonitrile ligand near δ 2.65. No evidence was found for the formation of diacetonitrile derivatives $\text{Os}_3(\text{CO})_9\text{-}(\text{CNR})(\text{NCMe})_2$ in CH_2Cl_2 even in the presence of a de-

(1) Kutty, D. W.; Alexander, J. J. *Inorg. Chem.* 1978, 17, 1489.

(2) Adams, R. D.; Golembeski, N. M. *J. Am. Chem. Soc.* 1979, 101, 2579.

(3) Lin, Y. W.; Gau, H. M.; Wen, Y. S.; Lu, K. L. *Organometallics* 1992, 11, 1445.

(4) Hardcastle, K. I.; McPhillips, T.; Arce, A. J.; Sanctis, Y. D.; Deeming, A. J.; Powell, N. I. *J. Organomet. Chem.* 1990, 389, 361.

(5) Arce, A. J.; Sanctis, Y. D.; Deeming, A. J. *Polyhedron* 1988, 7, 979.

[†] Academia Sinica.

[‡] National Chung-Hsing University.